NASA TECHNICAL MEMORANDUM

NASA TM X-52257

GPO PRICE $ _____

CFSTI PRICE(S) $ _____

Hard copy (HC) 1.00

Microfiche (MF) .50

ff 653 July 65

NASA TM X-52257

VORTEX VALVE PERFORMANCE POWER INDEX

by Vernon D. Gebben
Lewis Research Center
Cleveland, Ohio

TECHNICAL PAPER proposed for presentation at Symposium on Fluidics sponsored by the American Society of Mechanical Engineers and Harry Diamond Laboratories Layfayette, Indiana, May 8-10, 1967

NATIONAL AERONAUTICS AND SPACE ADMINISTRATION · WASHINGTON, D.C. · 1966

VORTEX VALVE PERFORMANCE POWER INDEX

by Vernon D. Gebben

Lewis Research Center
Cleveland, Ohio

TECHNICAL PAPER proposed for presentation at

Symposium on Fluidics
sponsored by the American Society of Mechanical Engineers
and Harry Diamond Laboratories
Lafayette, Indiana, May 8-10, 1967

NATIONAL AERONAUTICS AND SPACE ADMINISTRATION

VORTEX VALVE PERFORMANCE POWER INDEX

by Vernon D. Gebben

National Aeronautics and Space Administration
Lewis Research Center
Cleveland, Ohio

ABSTRACT

The pressure, flow, and power characteristics of a vortex valve are altered by changing the geometry of the unit. An index was developed for evaluating changes in the power consumption. This index is considered to be an important parameter which should be examined during the design of an optimized vortex valve. The power index is determined by the ratio of the maximum radial inlet power to the tangential inlet power required to stop the radial inlet flow. Characteristics and applications for the power index are illustrated by results from an experimental investigation.

Author

INTRODUCTION

Technology has produced a wide variety of applications for jet-driven vortices. Examples include the Ranque-Hilsch tube for energy separation, binary material distribution chamber for nuclear cavity reactor concepts, swirl atomizer used in fuel injectors and spraying equipment, magnetohydrodynamic generator, vortex diode, angular rate sensors, and the vortex class of fluid amplifiers. Common to these applications is the production and maintenance of their vortex flow patterns. Depending on the application, it is usually desired to minimize either the pressure, flow, or power required by the tangential driving jet. A performance index for evaluating the power supplied to the tangential driving jet is presented in this paper.

The index was developed for the vortex valve shown schematically in figure 1. The conventional vortex valve is a short cylindrical chamber with two inlets - a radial inlet and a tangential nozzle. The radial inlet allows the fluid to enter the chamber and flow to the outlet orifice without appreciable pressure drop. The tangential nozzle (or nozzles) injects the fluid tangentially along the cylindrical wall and thereby generates a vortex flow pattern. The fluid leaves the chamber through the outlet orifice located at the center of one or both end walls.

The vortex valve is a variable restrictor that modulates flow and amplifies signals in fluid circuits. The total flow leaving the vortex chamber is controlled by the amount of swirl imparted to the fluid inside the chamber. Typical outlet mass flow characteristics for a constant radial supply pressure are shown in figure 2. The maximum outlet flow (point R) occurs when the tangential nozzle flow is zero; a condition of no swirl in the chamber. The minimum outlet flow (point T) occurs when the vortex conditions prevent radial inlet flow. At point T the outlet and tangential nozzle mass flow rates are equal.

The power supplied at operating condition T, figure 2, will be related to a performance index. This "vortex valve power index" represents the potential power throttling ability of the valve. To illustrate the characteristics and applications for the index, the results from an experimental investigation are presented.

VORTEX VALVE POWER INDEX

The vortex valve power index is determined by pressure-flow measurements external to the valve. This type of performance number circumvents the problem of analyzing three-dimensional flow in the chamber caused by viscous phenomena. For example, observations and detailed measurements of confined

vortices have shown that the primary source of degraded performance results from inflow along the end walls (1-5); a phenomenon not indicated by inviscid flow theory. The effect is a short circuit path between the inlet and outlet. Mixing efficiency of the radial and tangential inlet flows, turbulence, secondary vortices, and three-dimensional sink flow add to the complexity of the vortex field (6-7). Consequently, the power index and other reported methods for analyzing the vortex valve are based on empirical models derived from input-output characteristics (8-14).

The power index is defined as the ratio of powers that would be available from two isentropic flow processes. The first is the isentropic power for the theoretical maximum outlet flow; operating condition R of figure 2. The other power is determined from measurements of the tangential nozzle flow during minimum outlet flow; condition T of figure 2. Mathematically, the power index for gas is expressed:

$$\text{Power Index} = \frac{(\dot{m}'_r)(\Delta h_r)}{(\dot{m}_t)(\Delta h_t)} \qquad (1)$$

where

$\dot{m}'_r$ = theoretical mass flow rate through the outlet orifice with unity discharge coefficient. Pressure differential across the orifice is the specified radial inlet pressure minus the specified exhaust pressure. The outlet area is considered to be extremely small compared to the radial inlet area.

$\dot{m}_t$ = measured tangential nozzle mass flow rate for the operating condition of zero radial inlet flow at the specified radial inlet pressure.

Δh_r = change in enthalpy for an isentropic flow process between the radial inlet and exhaust.

Δh_t = change in enthalpy for an isentropic flow process between the tangential nozzle inlet and exhaust during the operating condition of zero radial inlet flow at the specified radial inlet pressure.

For the isentropic flow process we have the following relationship:

$$\Delta h = \frac{RT_1}{\alpha}\left[1 - \left[\frac{P_2}{P_1}\right]^{\alpha}\right] \tag{2}$$

where

R = gas constant

T = temperature

P = pressure

$\alpha = (k - 1)/k$

k = ratio of specific heats

Subscripts 1 and 2 refer to the upstream and downstream conditions, respectively.

Generally, the same gas at equal temperature is supplied to both the radial inlet and the tangential nozzle. Therefore, for these conditions the power index can be defined:

$$\text{Power Index} = \left(\frac{\dot{m}_r'}{\dot{m}_t}\right)\left[\frac{1 - (P_e/P_r)^{\alpha}}{1 - (P_e/P_t)^{\alpha}}\right] \tag{3}$$

where

P_e = exhaust pressure (specified)

P_r = radial inlet supply pressure (specified)

P_t = tangential nozzle supply pressure

The numerator of equation (3) defines the theoretical power delivered to the valve when the tangential nozzle flow is zero. Its function is to normalize the denominator that represents the power supplied to the tangential nozzle for maintaining the radial inlet shutoff condition, point T of figure 2. An increase in the power index signifies an increase in efficiency because less power is required to stop the radial inlet flow. This convention is similar to the flow turndown quantity (10) that equals the ratio of maximum to minimum outlet mass flow rates as given by points R and T in figure 2.

Equation (3) can be rearranged in the following form:

$$\frac{\text{Power Index}}{(\dot{m}'_r/\dot{m}_t)} = \frac{1 - (P_e/P_r)^{\alpha}}{1 - \left[\dfrac{1}{\left(\dfrac{P_t - P_e}{P_r - P_e}\right)\left(\dfrac{P_r}{P_e} - 1\right) + 1}\right]^{\alpha}} \tag{4}$$

Equation (4) can be used for constructing nomograms that represent the functional relationship of the power index, flow turndown index, supply pressure ratio, and the control pressure ratio; where

Flow turndown index $= \dot{m}'_r/\dot{m}_t$

Supply pressure ratio $= P_r/P_e$

Control pressure ratio $= (P_t - P_e)/(P_r - P_e)$

In figure 3 the control pressure ratio and the supply pressure ratio establish values for the power-to-flow ratio on the ordinate. For example, a control pressure ratio of 1.5 and a supply pressure ratio of 2 results in a power-to-flow ratio of 0.78. The power index is then obtained from the product of the power-to-flow ratio and the flow turndown index. Figure 3 provides

a convenient method for determining the power index for various supply pressure ratios.

Figure 4 shows another graphical method for determining the power index. Flow turndown index versus control pressure ratio is plotted for various values of power index. In this example, the figure displays the characteristics for the specified supply pressure ratio of 0.74. The figure illustrates that, for a constant power index, an increase in the control pressure ratio results in an increase in the flow turndown. The map can also be used to determine an upper limit for the flow turndown index if (1) the power index is known and (2) upper limits for the tangential and radial supply pressures are specified.

The power index was developed for the vortex class of fluid amplifiers. However, it is expected that the power index will be useful in evaluating the performance of other types of vortex devices. For example, one may desire to minimize the tangential nozzle flow without increasing the power consumption or changing the chamber peripheral pressure in a device that contains no radial inlets. A modification in geometry may reduce the tangential nozzle flow but require a higher tangential nozzle supply pressure. The higher supply pressure, however, does not necessarily imply that the power consumption has increased. To evaluate the effects of the geometry change, the operating power must be computed from both pressure and flow rate values. For this application, the power index provides a convenient method. A constant power index represents no change in the power consumption. A lower number for the index signifies that higher power is supplied to the tangential nozzle; i.e., a decrease in efficiency.

EXPERIMENTAL INVESTIGATION

The effects of varying tangential nozzle area were investigated with the vortex chamber shown in figure 5. Results presented in this section illustrate an application for the power index.

The vortex chamber used in the experiments was constructed from two adjacent plates with semi-circular open sections that formed both the cylindrical wall of the chamber and two adjustable tangential nozzles. The chamber diameter was 2.54 cm (1 inch) and the distance between the end walls was 0.30 cm (0.12 inch). The end walls were flat and had a smooth surface of approximately 16 microinch finish. The tangential nozzles, located at the chamber periphery, had rectangular cross sections that extended between the end walls. The nozzle area was adjusted by the position of the two plates that formed the cylindrical wall. Because the unit contained no radial inlets, the pressure at the chamber periphery was used to represent radial inlet pressure during the condition of zero radial inlet flow. This peripherial pressure measurement was obtained from a pressure tap located in the cylindrical wall 90° downstream from a tangential nozzle. The outlet, located in one of the end walls, was an orifice with diameter of 0.358 cm (0.141 inch) and length of 0.05 cm (0.02 inch) followed by an axisymmetric 60° conical diffuser.

The supply media was air that varied in temperature between 77° and 81° F. Variations in the supply temperature were recorded but not used in the flow calculations. The outlet flow exhausted to the atmosphere. Pressures were measured with the following gages: 0 to 10 N/cm^2 gage (15 psig), 0 to 52 N/cm^2 gage (75 psig), 0 to 69 N/cm^2 gage (100 psig), and 0 to 3 N/cm^2 (4.5 psi) differential for pressures less than 10 N/cm^2 gage (15 psig). These were precision gages with errors less than 0.1 percent of full scale. Except

for the differential gage, the tangential nozzle supply pressure and the peripheral (radial inlet) pressure were measured with the same gage to eliminate errors due to small differences between gages. A calibrated rotameter in the supply line measured mass flow rate with errors estimated to be less than 1.5 percent of the actual value. The barometric pressure was recorded and used in computing the power index and the flow turndown index.

Figure 6 shows the effects of tangential nozzle area for a radial inlet pressure of 3.45 N/cm^2 gage (5 psig) in the upper plot and for 27.6 N/cm^2 gage (40 psig) in the lower plot. For the largest nozzle area tested, the pressure drop across the tangential nozzle ($P_t - P_p$) was very small, resulting in a control pressure ratio near unity. Consequently, the power index and flow turndown index for the largest nozzle area were nearly equal as indicated by equation (4). For the area range tested, a decrease in nozzle size resulted in an increase in both the flow turndown index and the control pressure ratio. The power index also increased as the size nozzle was reduced but it reached a maximum and then decreased when the nozzle area ratio (A_t/A_o) was reduced below 0.3 in the upper plot or below 0.2 in the lower plot. The decrease in power index for the smaller nozzles was probably caused by mixing losses in the chamber and viscous losses in the nozzle.

The configuration with the maximum power index is considered as the most efficient vortex valve. For the unit tested, the maximum power index occurred for a tangential nozzle geometry that had a control pressure ratio less than 1.5; a geometry within the range of conventional designs. It was also noted in the upper plot (fig. 6) that the flow turndown ratio had no distinct features for determining the most efficient vortex valve. The control pressure ratio and

the flow turndown index both affected the power index curve.

Figure 7 shows the effects of supply pressure. The upper plot was obtained from an element with a tangential to outlet area ratio of 0.169. Characteristics for a larger nozzle (area ratio of 0.615) are presented in the lower plot. In both cases flow turndown ratio increased appreciably for reduced pressures.

The characteristics shown in figures 6 and 7 were appreciably different from those predicted by a simplified model of an inviscid two-dimensional vortex. The power index, flow turndown index, and the control pressure ratio characteristics for the theoretical model illustrated in figure 8 are derived from the following relationships. The contribution to the pressure gradient by radial velocity component is small compared to the effect of the tangential velocity component. Therefore, the radial momentum equation reduces to

$$\frac{dP}{dr} - \rho \frac{v^2}{r} = 0 \tag{5}$$

The tangential momentum equation for zero axial flow is

$$\frac{dv}{dr} + \frac{v}{r} = 0 \tag{6}$$

For specified values for the effective chamber radius (r_p) and the effective outlet radius (r_o), equations (5) and (6) can be combined and simplified by the following functional relationship.

$$P_p - P_e = f(v_p^2) \tag{7}$$

In the theoretical model, the velocity from the nozzle (v_t) is considered equal to the tangential velocity component at the peripherial boundary. Therefore, equation (7) can be expressed

$$P_p - P_e = f(v_t^2) \tag{8}$$

For the tests described in this report, the velocity from the tangential nozzle was less than sonic. Under these conditions, the tangential nozzle velocity for an isentropic process is described by

$$v_t^2 = \frac{2\alpha P_t}{\rho_t}\left[1 - (P_p/P_t)^{\alpha}\right] \tag{9}$$

Combining equations (8) and (9), it follows that the value for the tangential nozzle supply pressure (P_t) is established when the peripheral pressure (P_p) and the exhaust pressure (P_e) are specified. Therefore, except for slight variations in the effective outlet radius resulting from changes in mass flow rate, the inviscid isentropic model shows that the tangential nozzle supply pressure (P_t) and the tangential nozzle velocity (v_t) are essentially independant of the tangential nozzle area.

From the characteristics of the simplified theoretical model, the following relationships are derived:

(a) Control pressure ratio is essentially independent of the tangential nozzle area;

(b) flow turndown index is essentially inversely proportional to the tangential nozzle area; and

(c) power index is essentially inversely proportional to the tangential nozzle area.

However, in figure 6, the control pressure ratio was not constant but increased appreciably when the tangential nozzle area decreased. The characteristics of the flow turndown index also deviated from the theoretical model; for example, an area change from 0.2 to 0.6 caused the flow turndown index to decrease by a factor of 1.3 instead of 3 in the theoretical case. The slope of the power index curve changed sign in figure 6, thus, displaying no correlation

to the theoretical. These large differences between theoretical and physical characteristics were considered to be caused by secondary flows not represented in the model.

CONCLUSION

Modifications in vortex valve geometry can increase or decrease both the operating pressure and flow rate of the tangential nozzle. To evaluate changes in the power efficiency of the unit, the power supplied to the tangential jet must be computed. The vortex valve power index defined in the report provides a useful and effective approach for comparing efficiencies of various vortex valves. It was concluded that the three normalized quantities representing pressure, flow, and power are all necessary in optimizing the steady state performance of vortex valves.

NOMENCLATURE

A	area
Δh	change in enthalpy for an isentropic flow process
k	ratio of specific heats
$\dot{m}$	measured mass flow rate
$\dot{m}'$	theoretical mass flow rate
P	pressure
r	radius
R	gas constant
T	temperature
v	velocity, tangential component
α	= (k - 1)/k
ρ	density

Subscripts

e	exhaust
o	outlet
p	conditions at chamber periphery
r	radial inlet
t	tangential nozzle
1	upstream conditions
2	downstream conditions

REFERENCES

1. O. L. Anderson, "Theoretical Solutions for the Secondary Flow on the End Wall of a Vortex Tube," United Aircraft Corp. Report No. R-2494-1, November, 1961.

2. A. C. Pinchak and R. Poplaswki, " On the Attainment of Extremely High Rotational Velocities in a Confined Vortex Flow," AIAA Paper No. 65-400, July, 1965.

3. R. Poplawski and A. C. Pinchak, "Aerodynamic Performance of Reversed Flow Vortex Chambers," Report No. ARL-65-219, AD-625405, United States Air Force, October, 1965.

4. D. H. Ross, "An Experimental Study of Secondary Flow in Jet-Driven Vortex Chambers," Report No. ATN-64(9227) - 1, AD-433052, Aerospace Corporation, January 27, 1964.

5. J. M. Savino and E. G. Keshock, "Experimental Profiles of Velocity Components and Radial Pressure Distributions in a Vortex Contained in a Short Cylindrical Chamber," NASA Technical Note D-3072, October, 1965.

6. C. D. Donaldson and G. G. Williamson, "An Experimental Study of Turbulence in a Driven Vortex," Technical Memo. 64-2, AD-609460, Aeronautical Research Associates of Princeton, Inc., July, 1964.

7. J. R. Weske and T. M. Rankin, "Production of Secondary Vortices in the Field of a Primary Vortex," Technical Note BN-244, AFOSR-623, University of Maryland, April, 1961.

8. E. A. Mayer and P. Maker, "Control Characteristics of Vortex Valves," Proceedings of Second Fluid Amplification Symposium, Harry Diamond Laboratories, May 26-28, 1964, Volume 2, pp. 61-84. (DDC No. AD-602001.)

9. L. B. Taplin, "Phenomenology of Vortex Flow and Its Application to Signal Amplification," Report No. RLDP 65-14, Rev. 1, Bendix Research Laboratories, October 1, 1965.

10. E. A. Mayer and L. B Taplin, "Vortex Devices," Fluidics, E. F. Humphrey, editor, Fluid Amplifier Associates, Boston, Massachusetts, 1965, pp. 185-200.

11. L. B. Taplin, "Small Signal Analysis of Vortex Amplifiers," Bendix Research Lab. Report included in the 2.73 course Notes, Department of Mechanical Engineering, Massachusetts Institute of Technology, July 1, 1966.

12. I. Greber, P. E. Koerper and C. K. Taft, "Fluid Vortex Amplifier Optimization," Proceedings of Third Fluid Amplification Symposium, Harry Diamond Laboratories, October 26-28, 1965, Volume 2, pp. 223-243. (DDC No. AD-623456.)

13. A. C. Bell, "Optimization of Vortex Valve," S. M. Thesis, Department of Mechanical Engineering, Massachusetts Institute of Technology, December, 1965.

14. D. N. Wormley, "Static Characteristics of Vortex Valve Pure Fluid Modulators," 2.73 course notes, Department of Mechanical Engineering, Massachusetts Institute of Technology, July, 1966.

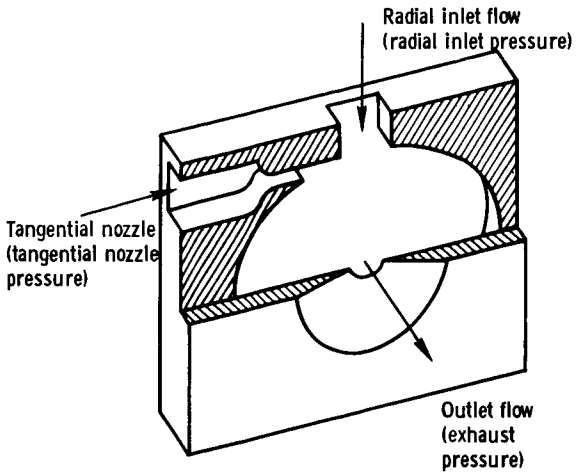

Figure 1. - Schematic illustration of the vortex valve.

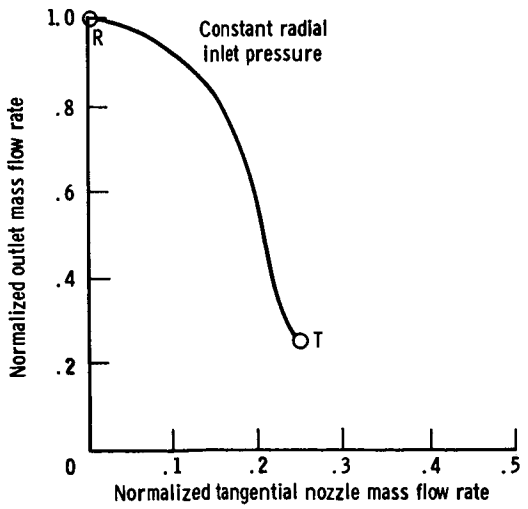

Figure 2. - Mass flow characteristics of a typical vortex valve.

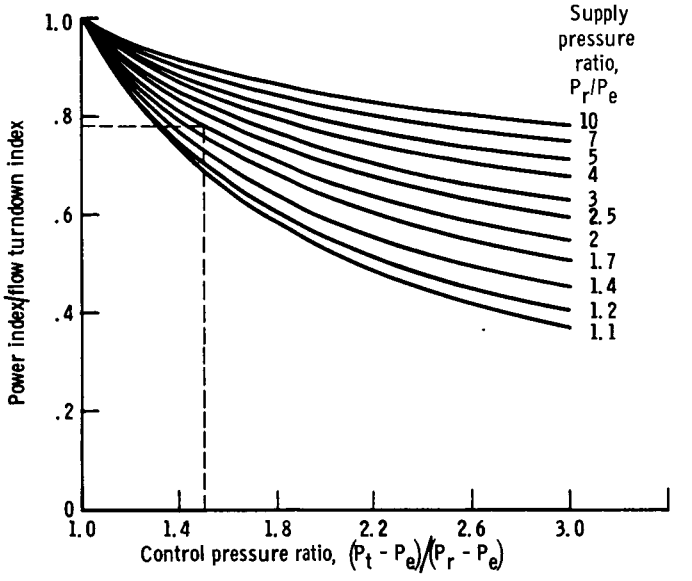

Figure 3. - Power index nomogram.

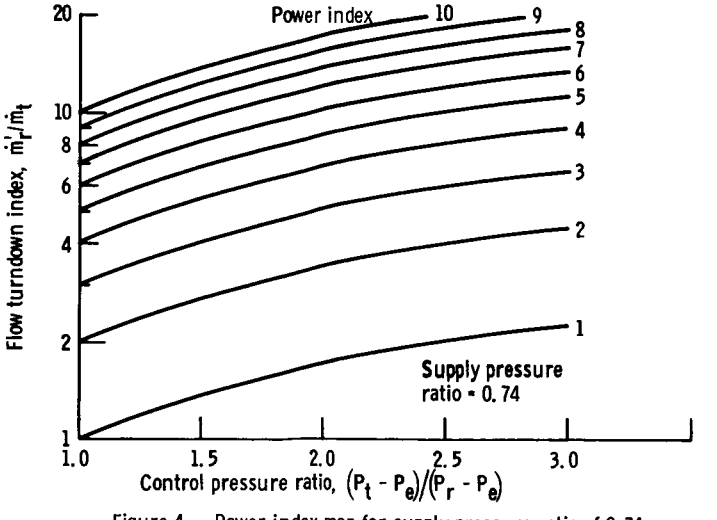

Figure 4. - Power index map for supply pressure ratio of 0.74.

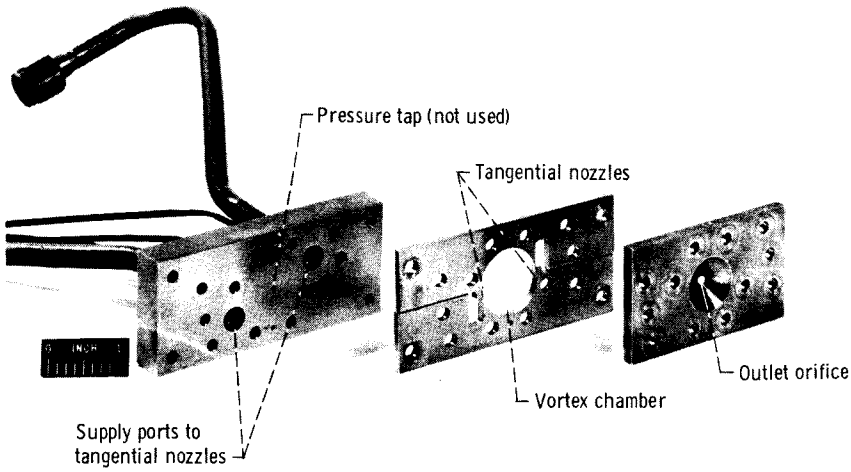

C-72067

Figure 5. - Vortex chamber display.

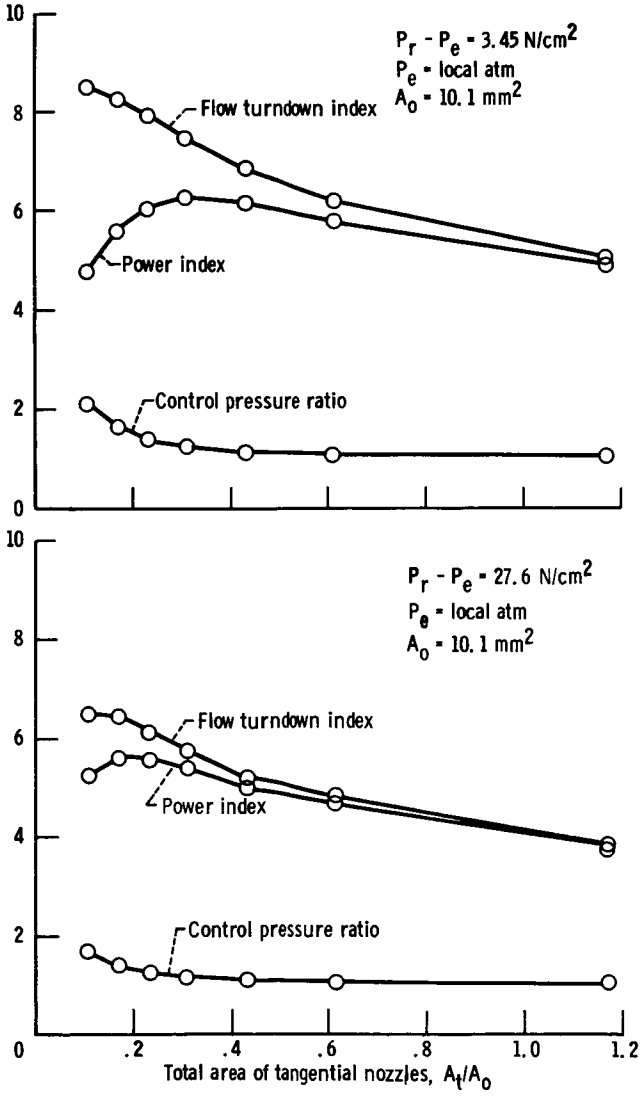

Figure 6. - Effects of tangential nozzle area.

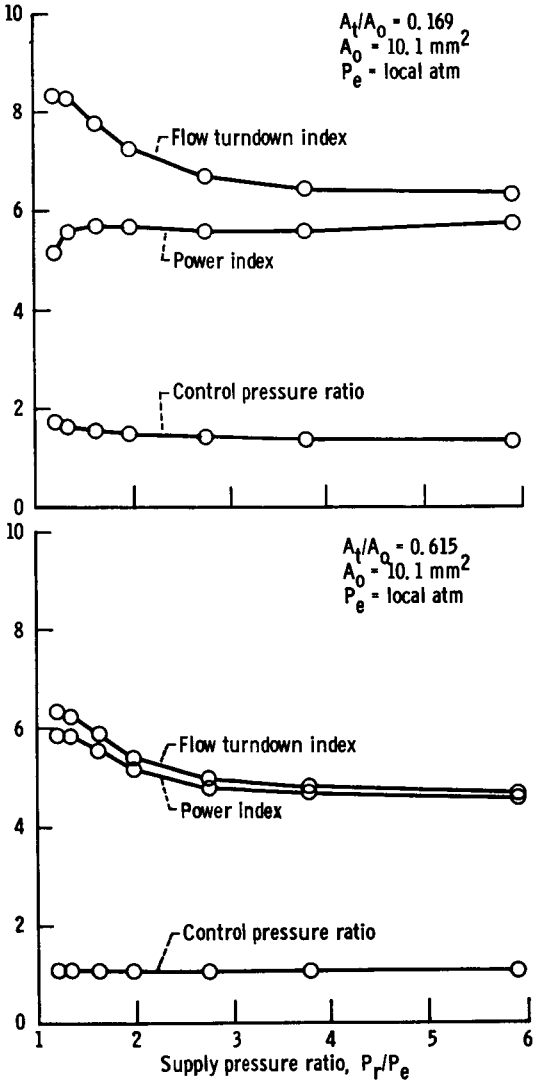

Figure 7. - Effects of supply pressure.

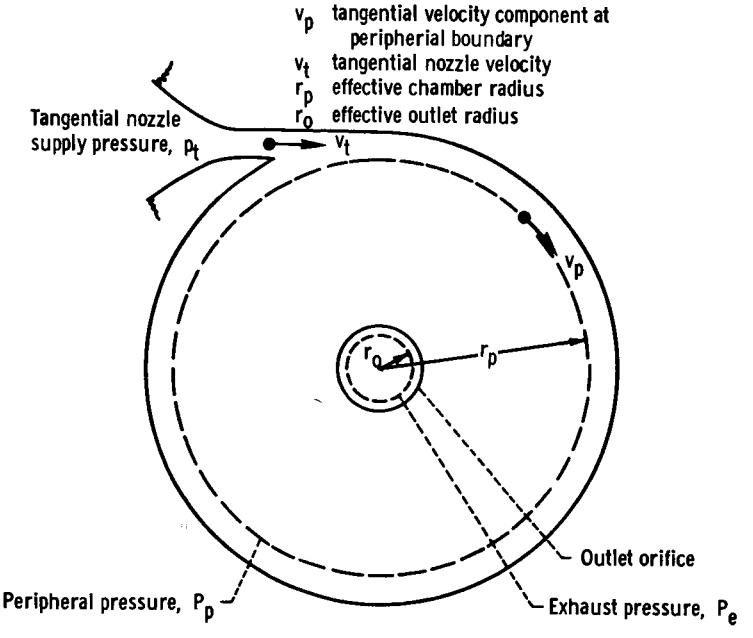

Figure 8. - Schematic illustration of the theoretical model geometry.